Density Functional Theory Study on Dimerizations of Phospholes†

T. C. Dinadayalane and G. Narahari Sastry*

Molecular Modeling Group, Organic Chemical Sciences, Indian Institute of Chemical Technology, Hyderabad-500 007, India

Received July 17, 2003

Dimerization reactions through [4 + 2] cycloadditions on 1*H*-, 2*H*-, and 3*H*-phospholes and cyclopentadiene were examined at the B3LYP level using 6-31G* and 6-311+G** basis sets. Activation energies for all the structures indicate that endo transition states are lower by about 1−4.5 kcal/mol compared to the corresponding exo transition states. While the transition-state stabilizations are controlled by secondary orbital interactions, the dimer stabilities are controlled by a mix of secondary orbital interactions and steric factors. Among the transition-state structures, **1-TS-endo**, ***syn*-1P-TS-endo**, **2P-TS-endo4**, and **3P-TS-endo2** are akin to bis-pericyclic transition-state structures and the rest are regular [4 + 2] cycloaddition transition states. Computational prediction of the facile dimerization of 2*H*-phospholes involving P···P bond formation is in agreement with Mathey's experimental observation. In comparison to the dimerization of cyclopentadiene, phosphole dimerizations involving the conversion of C═P to C−P are stabilized by about 10 kcal/mol. However, only when conversion of C═C is involved in the case of 1*H*-phosphole dimerizations, the activation energies are slightly higher. Further reactivities of dimers in the direction of cage formation or oligomerization are explored. The cage formation seems to be very feasible in 3*H*-phosphole dimers and very unlikely for 1*H*-phosphole dimers. Similarly, 1*H*- and 2*H*-phospholes are not expected to oligomerize further, and 3*H*-phospholes have a very high probability of oligomerization.

Introduction

Among the chemistries of five-membered heterocyclic compounds, that of phospholes is rather limited compared with those of pyrrole, furan, and thiophene.[1,2] However, soon after the discovery and unambiguous characterization of parent and substituted analogues,[3,4] the chemistry of phosphole has gained momentum, with notable contributions from Mathey's group.[1] Exploration of the structure, stability, aromaticity, and reactivity of phospholes is intrinsically interesting due to their unique nature and has generated meaningful interplay between theoretical and experimental studies.[3−17] Although both 1*H*- and 2*H*-phospholes were independently characterized,[3,4,8] 3*H*-phosphole is still elusive and is available only in the benzo-fused form, denoted as 3*H*-phosphaindene.[18] Phospholes and their Diels−Alder adducts exhibit novel modes of binding with transition-metal fragments, and phosphametallocenes have useful catalytic applications in olefin polymerizations.[19−22]

† IICT Communication No. 030607.

(1) Mathey, F. *Chem. Rev.* **1988**, *88*, 429.
(2) Bird, C. W. In *Comprehensive Heterocyclic Chemistry II*; Katritzky, A. R., Rees, C. W., Scriven, E. F. V., Eds.; Pergamon Press: Oxford, U.K., 1996; Vol. 2.
(3) (a) Leavitt, F. C.; Manuel, T. A.; Johnson, F. *J. Am. Chem. Soc.* **1959**, *81*, 3163. (b) Quin, L. D.; Bryson, J. G. *J. Am. Chem. Soc.* **1967**, *89*, 5984.
(4) Charrier, C.; Bonnard, H.; de Lauzon, G.; Mathey, F. *J. Am. Chem. Soc.* **1983**, *105*, 6871.
(5) (a) Mattmann, E.; Simonutti, D.; Ricard, L.; Mercier, F.; Mathey, F. *J. Org. Chem.* **2001**, *66*, 755. (b) Mattmann, E.; Mathey, F.; Sevin, A.; Frison, G. *J. Org. Chem.* **2002**, *67*, 1208.
(6) Nyulaszi, L. *Chem. Rev.* **2001**, *101*, 1229.
(7) (a) Mathey, F.; Mercier, F.; Charrier, C.; Fischer, J.; Mitschler, A. *J. Am. Chem. Soc.* **1981**, *103*, 4595. (b) Charrier, C.; Bonnard, H.; Mathey, F. *J. Org. Chem.* **1982**, *47*, 2376.
(8) de Lauzon, G.; Charrier, C.; Bonnard, H.; Mathey, F.; Fischer, J.; Mitschler, A. *J. Chem. Soc., Chem. Commun.* **1982**, 1272.
(9) (a) Mathey, F.; Mercier, F. *C. R. Acad. Sci. Paris, Ser. IIb* **1997**, *324*, 701. (b) Laporte, F.; Mercier, F.; Ricard, L.; Mathey, F. *Bull. Soc. Chim. Fr.* **1993**, *130*, 843. (c) Le Goff, P.; Mathey, F.; Ricard, L. *J. Org. Chem.* **1989**, *54*, 4754.
(10) Dinadayalane, T. C.; Geetha, K.; Sastry, G. N. *J. Phys. Chem. A* **2003**, *107*, 5479.
(11) (a) Geetha, K.; Dinadayalane, T. C.; Sastry, G. N. *J. Phys. Org. Chem.* **2003**, *16*, 298. (b) Geetha, K.; Sastry, G. N. *Ind. J. Chem. A* **2003**, *42A*, 11.
(12) (a) Dinadayalane, T. C.; Vijaya, R.; Smitha, A.; Sastry, G. N. *J. Phys. Chem. A* **2002**, *106*, 1627. (b) Vijaya, R.; Dinadayalane, T. C.; Sastry, G. N. *J. Mol. Struct. (THEOCHEM)* **2002**, *589−590*, 291.
(13) (a) Dinadayalane, T. C.; Sastry, G. N. *J. Chem. Soc., Perkin Trans. 2* **2002**, 1902. (b) Dinadayalane, T. C.; Punnagai, M.; Sastry, G. N. *J. Mol. Struct. (THEOCHEM)* **2003**, *626*, 247.
(14) Bachrach, S. M.; Perriott, L. *J. Org. Chem.* **1994**, *59*, 3394.
(15) (a) Bachrach, S. M. *J. Org. Chem.* **1994**, *59*, 5027. (b) Salzner, U.; Bachrach, S. M. *J. Organomet. Chem.* **1997**, *529*, 15.
(16) Bachrach, S. M.; Perriott, L. M. *Can. J. Chem.* **1996**, *74*, 839.
(17) Keglevich, G.; Nyulaszi, L.; Chuluunbaatar, T.; Namkhainyambuu, B.-A.; Ludanyi, K.; Imre, T.; Toke, L. *Tetrahedron* **2002**, *58*, 9801.
(18) Aitken, R. A.; Clasper, P. N.; Wilson, N. J. *Tetrahedron Lett.* **1999**, *40*, 5271.
(19) Vlaar, M. J. M.; de Kanter, F. J. J.; Schakel, M.; Lutz, M.; Spek, A. L.; Lammertsma, K. *J. Organomet. Chem.* **2001**, *617−618*, 311.
(20) Keglevich, G.; Kegl, T.; Chuluunbaatar, T.; Dajka, B.; Matyus, P.; Balogh, B.; Kollar, L. *J. Mol. Catal. A* **2003**, *200*, 131.
(21) (a) Mathey, F. *J. Organomet. Chem.* **2002**, *646*, 15. (b) Janiak, C.; Versteeg, U.; Lange, K. C. H.; Weimann, R.; Hahn, E. *J. Organomet. Chem.* **1995**, *501*, 219. (c) de Boer, E. J. M.; Gilmore, I. J.; Korndorffer, F. M.; Horton, A. D.; van der Linden, A.; Royan, B. W.; Ruisch, B. J.; Schoon, L.; Shaw, R. W. *J. Mol. Catal. A* **1998**, *128*, 155. (d) Brown, S. J.; Gao, X.; Harrison, D. G.; Koch, L.; Spence, R. E. v. H.; Yap, G. P. A. *Organometallics* **1998**, *17*, 5445. (e) Salzner, U.; Lagowski, J. B.; Pickup, P. G.; Poirier, R. A. *Synth. Met.* **1998**, *96*, 177.

10.1021/om0340490 CCC: $25.00
Publication on Web 11/25/2003

Phospholes containing transition-metal fragments were also found to have potential applications in homogeneous catalysis such as hydrogenation, carbonylation, and hydroformylation reactions as well as in asymmetric synthesis.[22]

Mathey's group reported a higher stereospecific and facile dimerization of 2*H*-phosphole (**2P**) to yield an endo dimer containing a P−P bond, and also independently the ability of 2*H*-phospholes to act as a good diene and dienophile was demonstrated.[4,8,23] The elegant experimental studies demonstrated the reversible equilibration of the 2*H*-phosphole (**2P**) dimerization process through trapping of the monomer unit as a Diels−Alder adduct of acetylene.[4,8] Although the parent 1*H*-phosphole (**1P**) dimerization has not yet been reported, the cyclodimerizations of substituted 1*H*-phospholes as well as phosphole oxides and sulfides are known.[24−27] The exo and endo selectivity of Diels−Alder reactions and the involvement of secondary orbital interactions have generated interest recently, especially in the dimerization of cyclopentadiene and cyclopentadienone systems.[28] The experimental studies reported that the photochemical [2 + 2] intramolecular cycloaddition of endo Diels−Alder adducts of cyclopentadienone, P−P bonded 2*H*-phosphole dimer, and pentachlorinated cyclopentadiene yielded attractive cage compounds.[4,26,29] The foregoing discussion clearly indicates that cycloaddition reactions, sigmatropic shifts, and polymerization reactions are the primary reaction channels of phospholes. Several theoretical studies were reported in the literature to model the Diels−Alder reactions of phospholes, with varying dienophiles, and their sigmatropic rearrangements.[10−16] However, the dimerization energies appear to be of crucial importance in determining the isolation of phospholes. However, to our knowledge, there has been no theoretical study on the dimerization of phospholes.

Considering the immense interest in the reactions of phospholes, the present paper aims to study the dimerization processes of 1*H*-, 2*H*-, and 3*H*-phospholes in detail, and the dimerization of cyclopentadiene is also included for comparison. Previous theoretical studies have revealed the limitations of traditional HF and MP2 approaches to obtain the activation energies for the Diels−Alder reactions and other cycloaddition reactions, and therefore the B3LYP method was employed, which proved to be reliable.[12,30] The present study reports the transition-state structures and products for all the possible dimers of the dienes considered (Chart 1). Frontier molecular orbital analysis is used to explain the computed activation barriers. Further, the possibility for the oligomerization of the dimers of phospholes as well as the cage formation is explored. Thus, this paper provides a systematic computational study for the first time on phosphole dimerizations and a few thoughts on further reactions.

Chart 1

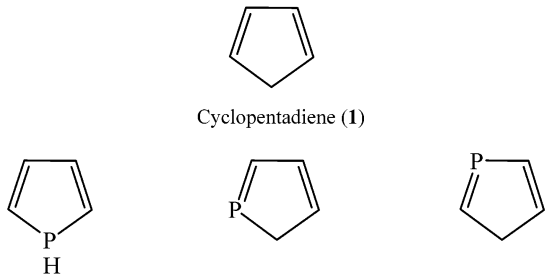

Computational Methods

The reactants, transition states, and products for all the possible dimers of the 1*H*-, 2*H*-, and 3*H*-phospholes (**1P**−**3P**) obtained through [4 + 2] cycloaddition reactions were optimized and characterized using the hybrid density functional theory method B3LYP with a 6-31G* basis set. For comparison of the results, the calculations were also performed for the dimerization reactions of cyclopentadiene at the same level of theory. The frequency calculations indicate that all the products are minima and the transition states possess one imaginary frequency. The normal modes corresponding to the imaginary frequency in all the transition-state structures were verified through the MOPLOT program package.[31] The B3LYP/6-31G* calculations were performed for the cage compounds, characterized as minima, obtained from the endo products via [2 + 2] addition. The single-point calculations at the B3LYP/6-311+G** level on B3LYP/6-31G* geometries were carried out uniformly for all the species considered in the study. HF/6-31G* calculations on B3LYP geometries were done for all the reactants and products to calculate the FMO energies and HOMO−LUMO energy gaps. All the calculations were performed using the Gaussian 98 suite of programs.[32]

Results and Discussion

Equilibrium Geometries. The [4 + 2] addition of cyclopentadiene with one of the double bonds of another cyclopentadiene affords both exo and endo adducts

(22) (a) Mathey, F.; Mercier, F.; Robin, F.; Ricard, L. *J. Organomet. Chem*. **1998**, *577*, 117. (b) Wilkes, L. M.; Nelson, J. H.; McCusker, L. B.; Seff, K.; Mathey, F. *Inorg. Chem*. **1983**, *22*, 2476. (c) Choudary, B. M.; Reddy, N. P.; Jamil, M. Z. *Polyhedron* **1986**, *5*, 911. (d) Loh, S.-K.; Vittal, J. J.; Leung, P.-H. *Tetrahedron: Asymmetry* **1998**, *9*, 423.

(23) de Lauzon, G.; Charrier, C.; Bonnard, H.; Mathey, F. *Tetrahedron Lett*. **1982**, *23*, 511.

(24) Delaere, D.; Nguyen, M. T.; Vanquickenborne, L. G. *J. Organomet. Chem*. **2002**, *643*−*644*, 194.

(25) Keseru, G. M.; Keglevich, G. *J. Organomet. Chem*. **1999**, *586*, 166.

(26) Marchand, A. P.; Ganguly, B.; Malagon, C. I.; Lai, H.; Watson, W. H. *Tetrahedron* **2003**, *59*, 1763.

(27) (a) Keglevich, G.; Chuluunbaatar, T.; Ludanyi, K.; Toke, L. *Tetrahedron* **2000**, *56*, 1. (b) Quin, L. D.; Mesch, K. A. *J. Chem. Soc., Chem. Commun*. **1980**, 959. (c) Mathey, F.; Mercier, F. *Tetrahedron Lett*. **1981**, *22*, 319.

(28) (a) Caramella, P.; Qadrelli, P.; Tomo, L. *J. Am. Chem. Soc*. **2002**, *124*, 1130. (b) Qadrelli, P.; Romano, S.; Toma, L.; Caramella, P. *J. Org. Chem*. **2003**, *68*, 6035.

(29) Tomioka, H.; Hirano, Y.; Izawa, Y. *Tetrahedron Lett*. **1974**, *15*, 4477.

(30) (a) Goldstein, E.; Beno, B.; Houk, K. N. *J. Am. Chem. Soc*. **1996**, *118*, 6036. (b) Beno, B. R.; Wilsey, S.; Houk, K. N. *J. Am. Chem. Soc*. **1999**, *121*, 4816. (c) Jursic, B.; Zdravkovski, Z. *J. Chem. Soc., Perkin Trans. 2* **1995**, 1223. (d) Jorgensen, W. L.; Lim, D.; Blake, J. F. *J. Am. Chem. Soc*. **1993**, *115*, 2936.

(31) Bally, T.; Albrecht, B.; Matzinger, S.; Sastry, G. M. MOPLOT 3.2; University of Fribourg, 1997.

(32) Frisch, M. J.; Trucks, G. W.; Schlegel, H. B.; Scuseria, G. E.; Robb, M. A.; Cheeseman, J. R.; Zakrzewski, V. G.; Montgomery, J. A., Jr.; Stratmann, R. E.; Burant, J. C.; Dapprich, S.; Millam, J. M.; Daniels, A. D.; Kudin, K. N.; Strain, M. C.; Farkas, O.; Tomasi, J.; Barone, V.; Cossi, M.; Cammi, R.; Mennucci, B.; Pomelli, C.; Adamo, C.; Clifford, S.; Ochterski, J.; Petersson, G. A.; Ayala, P. Y.; Cui, Q.; Morokuma, K.; Rega, N.; Salvador, P.; Dannenberg, J. J.; Malick, D. K.; Rabuck, A. D.; Raghavachari, K.; Foresman, J. B.; Cioslowski, J.; Ortiz, J. V.; Baboul, A. G.; Stefanov, B. B.; Liu, G.; Liashenko, A.; Piskorz, P.; Komaromi, I.; Gomperts, R.; Martin, R. L.; Fox, D. J.; Keith, T.; Al-Laham, M. A.; Peng, C. Y.; Nanayakkara, A.; Challacombe, M.; Gill, P. M. W.; Johnson, B. G.; Chen, W.; Wong, M. W.; Andres, J. L.; Gonzalez, C.; Head-Gordon, M.; Replogle, E. S.; Pople, J. A.; *Gaussian 98*, Revision A.11.2; Gaussian, Inc., Pittsburgh, PA, 2001.

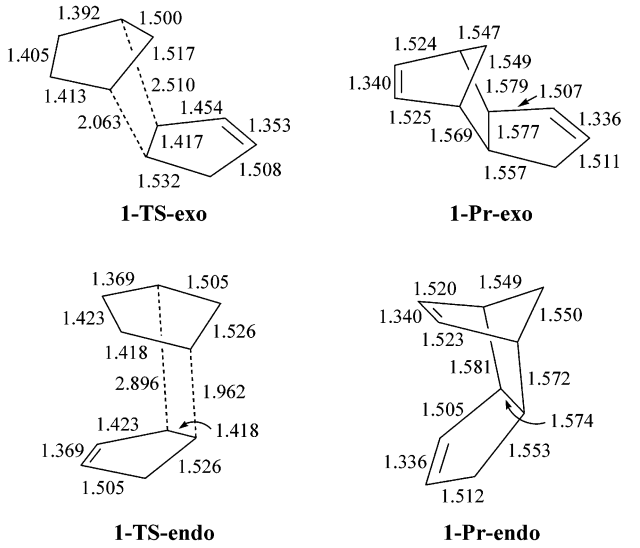

Figure 1. B3LYP/6-31G* optimized geometries of the transition states and products of the cyclopentadiene (**1**) cyclodimerizations. The bond lengths are given in Å.

through the corresponding transition states. Optimized structures with principal geometric parameters for the transition states and products are depicted in Figure 1. The bond lengths of the exo and endo fused products are quite similar. The deviations in the transition-state C···C bond lengths are about 0.45 and 0.9 Å in **1-TS-exo** and **1-TS-endo**, respectively. This indicates that reaction profiles are significantly nonsynchronous, although they are concerted. The transition-state C···C bond length, which is next to the sp^3 carbon of the dienophile moiety, is shorter than the other C···C bond length in both cases.

Among the possible products and transition states for [4 + 2] cyclodimerization of **1P**, four products are considered and their corresponding transition states were located and characterized at the B3LYP/6-31G* level. The orientation of hydrogen attached to phosphorus is considered only in diene and not in the dienophile. The optimized structures along with the bond lengths are depicted in Figure 2; syn and anti nomenclature is used to designate the orientation of phosphole hydrogen in diene away from and towards the incoming dienophile, respectively. Figure 2 indicates that the bond lengths are very similar in all four isomeric products. Except for the C···C bond lengths, there are no significant deviations in bond lengths between exo and endo transition states in both syn and anti forms. The C···C bond length, which is adjacent to the P atom of the dienophile moiety, is consistently shorter in exo and endo transition states compared to the other C···C bond length.

The cyclodimerization of **2P**, wherein the C═P part acts as a dienophile, results in four isomeric products by both exo and endo approaches. Similarly, the addition of **2P** across C═C of another **2P** gives a pair each for the exo and endo products. Figure 3 depicts the important geometric parameters for all the transition states and products of **2P** dimerizations. Figure 3 shows that bond lengths are very similar in the exo and endo products. However, a deviation of about 0.01 Å is observed for P−P and some of the P−C bond lengths between exo and endo products in 1 and 2. As it has been noted in case of 1*H*-phosphole, the transition-state structures show substantial nonsynchronous nature. Owing to the longer transition-state P···P bond length, the C···C bond lengths are longer compared to typical transition-state bond lengths in **2P-TS-exo1** and **2P-TS-endo1**. The intermolecular P···P and C···C bond lengths are shorter by about 0.12 and 0.02 Å in the endo transition state compared to the exo transition state, which points to a secondary orbital interaction (see the Supporting Information). The P···C bond lengths range from 2.56 to 2.96 Å in the transition states **2P-TS-exo2** and **2P-TS-endo2**. An examination of the transition-state structures **2P-TS-exo3** and **2P-TS-endo3** indicates that C···C bond lengths are longer than P···C bond lengths, clearly indicating high asynchronicity of the reactions. The transition-state bond lengths indicate that **2P-TS-exo4** seems to be a tighter transition state than **2P-TS-endo4**.

The [4 + 2] cyclodimerization of **3P** can afford eight products through eight different transition states. All

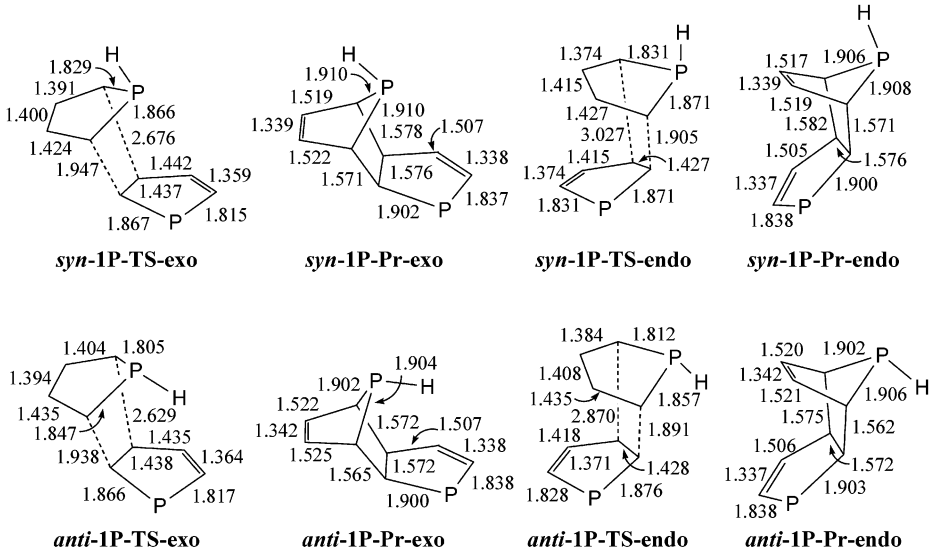

Figure 2. B3LYP/6-31G* optimized geometries of the transition states and products of the **1P** cyclodimerizations. The bond lengths are given in Å.

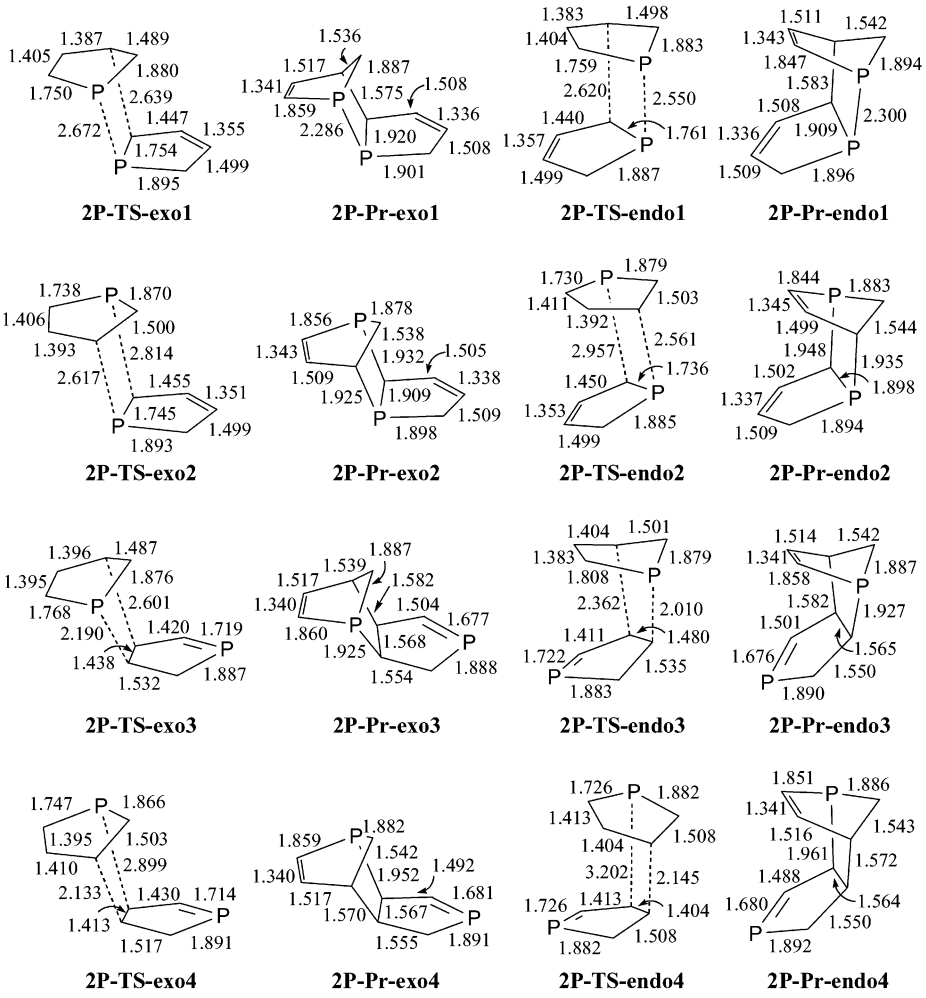

Figure 3. B3LYP/6-31G* optimized geometries of the transition states and products of the **2P** cyclodimerizations. The bond lengths are given in Å.

the products and transition-state geometries are depicted in Figure 4.[33] Figure 4 indicates that the transition states are unsymmetrical in nature and the bond lengths in exo and endo products are virtually similar. The C···P bond lengths range from 2.49 to 3.14 Å in **3P-TS-exo1**, **3P-TS-endo1**, **3P-TS-exo2**, and **3P-TS-endo2**. Except in the transition states **3P-TS-exo3** and **endo3**, the deviations in the intermolecular transition-state bond lengths between exo and endo transition states are about 0.06−0.27 Å. The transition-state C···P bond lengths are shorter in **exo1** and **endo1** transition states compared to **exo2** and **endo2**, while the C···C bond lengths show the opposite trend.

It is interesting to observe that among all the transition state structures obtained, in the structures ***syn*-1P-TS-endo**, **2P-TS-endo4**, and **3P-TS-endo2** the two phosphole fragments have very similar bond lengths. These transition states are very similar to the endo transition state (**1-TS-endo)** obtained for cyclopentadiene dimerization. The above four transition-state structures are akin to the bis-pericyclic transition states[28] and are favored by Salem−Houk type secondary orbital interactions.[34] Thus, in these structures, it is not possible to classify the reactant pair into diene and dienophile.

Activation and Reaction Energies. The activation energies obtained at the B3LYP level using 6-31G* and 6-311+G** basis sets for the cyclodimerizations of phospholes as well as for the cyclopentadiene are given in Table 1 along with the enthalpy and Gibbs free energies of activations. Jorgensen et al. studied the cyclodimerization reactions of cyclopentadiene at various levels of theory, and they reported that the MP3 method is good for obtaining reliable activation energies.[30d] The experimental activation barrier for the cyclopentadiene dimerization is 15.5 kcal/mol.[35] The present study indicates that B3LYP results are closer to the experimental results compared to the results for the MP2 method,[30d] and interestingly, 6-31G* values are better than those obtained with the 6-311+G** basis set. Despite the better agreement with the 6-31G* basis set, we resorted to performing B3LYP/6-311+G** calculations, as the method is expected to provide better energetics on a large number of reactant pairs. Table 1 shows that Gibbs free energies of activation follow the activation energies, and thus, the activation energies are taken for discussion. Endo transition states enjoy

(33) Several attempts made to locate the transition state **3P-TS-endo3** at the B3LYP level were in vain. Only the PM3 level of theory facilitated location of the correct transition-state structure which was used for single-point calculations.

(34) (a) Salem, L. *J. Am. Chem. Soc.* **1968**, *90*, 553. (b) Birney, D. M.; Houk, K. N. *J. Am. Chem. Soc.* **1990**, *112*, 4127.

(35) Benford, G. A.; Wassermann, A. *J. Chem. Soc.* **1939**, 362.

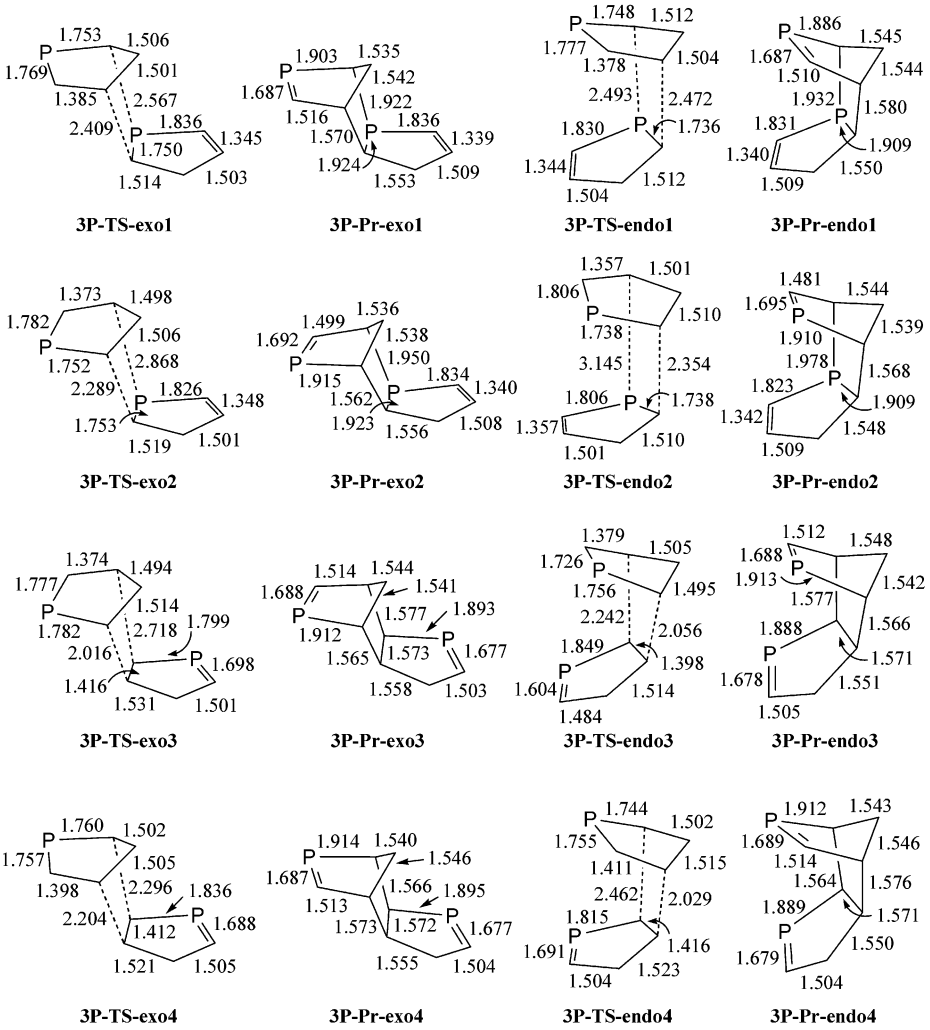

Figure 4. B3LYP/6-31G* optimized geometries of the transition states and products of the **3P** cyclodimerizations. The bond lengths are given in Å. The PM3 optimized structure and bond lengths are given for **3P-TS-endo3**.

favorable secondary orbital interactions (see the Supporting Information) in the range of 1−4.5 kcal/mol and average about 2 kcal/mol.

The cyclodimerizations of **1P** require higher activation energies compared to the dimerization reactions of other phospholes and the cyclopentadiene. This may be attributed to the aromaticity of 1*H*-phosphole (**1P**). In the dimerizations of **2P**, the reactions of **2P** addition across C═P resulting in P−P-bonded products require activation barriers of 3−5 kcal/mol, which are very low among all the possible dimerizations considered. This is followed by reactions that lead to cycloadducts containing two newly formed P−C bonds. The low activation energy for these reactions may be attributed to the breaking of two weak P═C bonds during the course of the reaction. The cycloaddition reactions of **2P** across the C═C bond of another **2P** require a considerably higher activation barrier, by about 7−13 kcal/mol, than the reactions across C═P. **2P-TS-endo3** and **2P-TS-endo4** lie about 4 kcal/mol below their corresponding exo transition states. However, the energy difference between exo and endo transition states is less than 2 kcal/mol in **2P** dimerizations, where the dienophile fragment is C═P.

Similar to **2P** dimerizations, the [4 + 2] addition of **3P** with C═P of another **3P** requires a lower barrier than the addition across C═C, indicating that addition across weaker double bonds is easier. The transition states **3P-TS-endo1** and **3P-TS-endo2** lie lower in energy by about 3 and 4.5 kcal/mol than their corresponding exo transition states. However, the reactions for the formation of **3P-Pr-exo4** and **3P-Pr-endo4** possess very similar activation energies. As two transition states and two products are expected for the dimerization of **3P**, where C═C acts as the dienophile, all the attempts to locate **3P-TS-endo3** were futile and the putative transition-state structures collapsed to **3P-TS-endo1**. In the attempts toward **3P-TS-endo3**, P═C can readily act as the dienophile rather than C═C, due to the favorable endo orientation, yielding **3P-TS-endo1**. In contrast to **2P** dimerizations, the diene **3P** possessing C═P breaks and simultaneously forms in the products of **3P** dimers. The lower activation barriers for the cycloaddition of **3P** across C═P of another **3P** may be attributed to the conversion of the weak dienophile C═P bond into C−P in the product. Cycloadditions of **3P** wherein C═C acts as the dienophile require an activation energy almost equal to or higher than the barrier required for the hydrocarbon analogue. The present study indicates that the activation energies are lower by about 8−10 kcal/mol for the reaction in which a C═P bond is converted into C−P compared to the hydrocarbon analogue. Therefore, the

Table 1. Activation Energies ($\Delta E^{\ddagger}$), Enthalpies ($\Delta H^{\ddagger}$), and Gibbs Free Energies ($\Delta G^{\ddagger}$) of Activations Obtained at the B3LYP/6-31G* Level and Activation Energies Obtained at the B3LYP/6-311+G Level for the Dimerization Reactions of 1 and 1P−3P[a]**

	B3LYP/6-31G*			B3LYP/
	$\Delta E^{\ddagger}$	$\Delta H^{\ddagger}$	$\Delta G^{\ddagger}$	6-311+G**[b] $\Delta E^{\ddagger}$
1-TS-exo	22.2	23.3	36.3	25.3
1-TS-endo	19.4	20.4	33.2	22.1
***syn*-1P-TS-exo**	29.1	29.7	43.2	31.6
***syn*-1P-TS-endo**	26.0	26.5	39.9	28.4
***anti*-1P-TS-exo**	26.8	27.7	41.5	29.2
***anti*-1P-TS-endo**	25.8	26.5	40.0	28.0
2P-TS-exo1	4.0	4.8	18.4	5.0
2P-TS-endo1	2.3	3.2	17.1	3.2
2P-TS-exo2	5.5	6.3	19.7	6.6
2P-TS-endo2	4.2	5.1	18.3	5.1
2P-TS-exo3	12.5	13.5	27.4	14.3
2P-TS-endo3	7.9	9.4	24.2	10.2
2P-TS-exo4	13.7	15.0	28.6	16.2
2P-TS-endo4	9.9	11.2	24.9	12.1
3P-TS-exo1	14.2	15.2	28.6	16.4
3P-TS-endo1	11.4	12.5	25.9	13.5
3P-TS-exo2	13.1	14.2	27.5	15.4
3P-TS-endo2	8.5	9.7	23.0	10.8
3P-TS-exo3	22.3	23.5	37.1	24.9
3P-TS-endo3	23.7[c]			26.9[c]
3P-TS-exo4	25.1	26.4	40.2	27.9
3P-TS-endo4	25.2	26.4	40.0	27.6

[a] All values are in kcal/mol. [b] Single-point calculations done on B3LYP/6-31G* geometries. [c] On PM3 geometries.

Table 2. Reaction Energies (ΔE_r), Enthalpies (ΔH_r), and Gibbs Free Energies (ΔG_r) of Reactions at the B3LYP/6-31G* Level and Reaction Energies at the B3LYP/6-311+G Level Obtained for the Dimerizations of 1 and 1P−3P[a]**

	B3LYP/6-31G*			B3LYP/
	ΔE_r	ΔH_r	ΔG_r	6-311+G**[b] ΔE_r
1-Pr-exo	−17.4	−13.4	0.9	−10.9
1-Pr-endo	−16.3	−12.3	2.0	−9.8
***syn*-1P-Pr-exo**	−7.3	−4.0	11.0	−2.1
***syn*-1P-Pr-endo**	−8.5	−5.2	9.8	−3.4
***anti*-1P-Pr-exo**	−9.5	−6.2	9.0	−4.3
***anti*-1P-Pr-endo**	−10.6	−7.3	7.7	−5.2
2P-Pr-exo1	−25.7	−22.5	−7.8	−22.2
2P-Pr-endo1	−23.5	−20.3	−5.5	−19.9
2P-Pr-exo2	−21.1	−18.4	−3.6	−18.7
2P-Pr-endo2	−20.2	−17.5	−2.7	−17.9
2P-Pr-exo3	−13.5	−10.3	4.3	−9.8
2P-Pr-endo3	−13.2	−9.9	4.9	−9.5
2P-Pr-exo4	−15.0	−11.7	3.1	−11.3
2P-Pr-endo4	−14.5	−11.2	3.7	−10.7
3P-Pr-exo1	−23.9	−20.2	−5.3	−18.9
3P-Pr-endo1	−22.2	−18.6	−3.6	−17.3
3P-Pr-exo2	−24.3	−20.7	−5.7	−19.2
3P-Pr-endo2	−23.4	−19.8	−4.8	−18.2
3P-Pr-exo3	−17.2	−13.1	1.8	−11.4
3P-Pr-endo3	−15.7	−11.6	3.4	−9.6
3P-Pr-exo4	−17.5	−13.3	1.7	−11.7
3P-Pr-endo4	−15.9	−11.8	3.3	−9.9

[a] All values are in kcal/mol. [b] Single-point calculations done on B3LYP/6-31G* geometries.

high reactivities of phospholes can be directly traced to the weaker C═P.

Table 2 lists the reaction energies, enthalpies, and Gibbs free energies of reactions for the cyclodimerizations considered. The reaction exothermicities are lower at the B3LYP/6-311+G** level compared to the B3LYP/6-31G* level, but the trends obtained at both levels are the same. Similar to the trends observed in activation energies, the exothermicities for the dimerizations of **1P** are consistently lower compared to dimerizations of **2P**, **3P**, and **1**. In the cases of **2P** and **3P** dimerizations, the reactions wherein C═P acts as dienophile are more exothermic by about 8−10 kcal/mol compared to the reactions involving C═C as dienophile. The activation and reaction energies reveal that C═P has a higher propensity to be the dienophile part compared to that of C═C, which is in agreement with the previous experimental and computational studies.[4,15] In **1P** dimerization, endo products are more stable by about 1 kcal/mol than exo products, indicating that secondary orbital interactions play a role not only in the transition states but also in the products. Computational studies on the dimerization of related species, phosphole 1-oxide dimers, also show similar trends.[25] In contrast to **1P** dimers, the exo products are more stable than endo products in **2P** and **3P** and also in cyclopentadiene dimers, indicating that the exo selectivity is preferred over endo in these cases. The higher selectivity of the exo product is due to overriding steric factors. The formation of the P−P-bonded **2P** dimers requires very low activation energy, and the reaction is more exothermic compared to other **2P** dimerizations. The present computational study supports Mathey's experimental observation that 2*H*-phosphole (**2P**) dimerization leads to a directly P−P bonded endo dimer, which on heating yielded the thermodynamic exo dimer.[4] The reactions of **3P** across C═P are more exothermic by about 7−9 kcal/mol than the reactions of **2P** across C═C.

Table 3. Activation and Reaction Energies for the Diels−Alder Reactions of 1P, 2P, and 3P with Ethylene and Acetylene as Dienophiles[a]

	ethylene				acetylene			
	B3LYP/ 6-31G*[b]		B3LYP/ 6-311+G**[c]		B3LYP/ 6-31G*[b]		B3LYP/ 6-311+G**[c]	
diene	$\Delta E^{\ddagger}$	ΔE_r	$\Delta E^{\ddagger}$	ΔE_r	$\Delta E^{\ddagger}$	ΔE_r	$\Delta E^{\ddagger}$	ΔE_r
1P								
syn	24.4	−19.3	27.4	−13.3	25.1	−30.7	28.7	−23.0
anti	24.6	−21.5	27.3	−15.2	26.1	*d*	29.2	*d*
2P	10.3	−27.7	12.6	−22.7	12.0	−38.4	14.7	−31.2
3P	20.4	−27.0	23.4	−20.3	21.4	−38.4	25.0	−29.9

[a] All values are in kcal/mol. [b] The values are taken from ref 10. [c] Single-point calculations were done on B3LYP/6-31G* geometries. [d] Only one product is possible due to the symmetry.

For comparison, the activation and reaction energies obtained for the Diels−Alder reactions of phospholes with both ethylene and acetylene as dienophiles are given in Table 3. The B3LYP/6-311+G** computed activation energy for the conversion of **1P** to **2P** through a [1,5]-sigmatropic shift is 18.3 kcal/mol, which is lower than the barriers for the cyclodimerization of **1P** and the Diels−Alder reactions of **1P** with the dienophiles (Tables 1 and 3). Thus, **1P** will undergo a sigmatropic shift to give **2P** rather than cyclodimerization or Diels−Alder reactions with dienophiles. This study indicates that a [1,5]-sigmatropic shift is the most feasible process in **1P**, and it takes place prior to either Diels−Alder or dimerization reactions. The activation energy for the sigmatropic shifts computed at the B3LYP/6-311+G** level for **2P** to **3P** and **3P** to **2P** conversions are 28.1 and 24.1 kcal/mol, respectively. The activation barriers

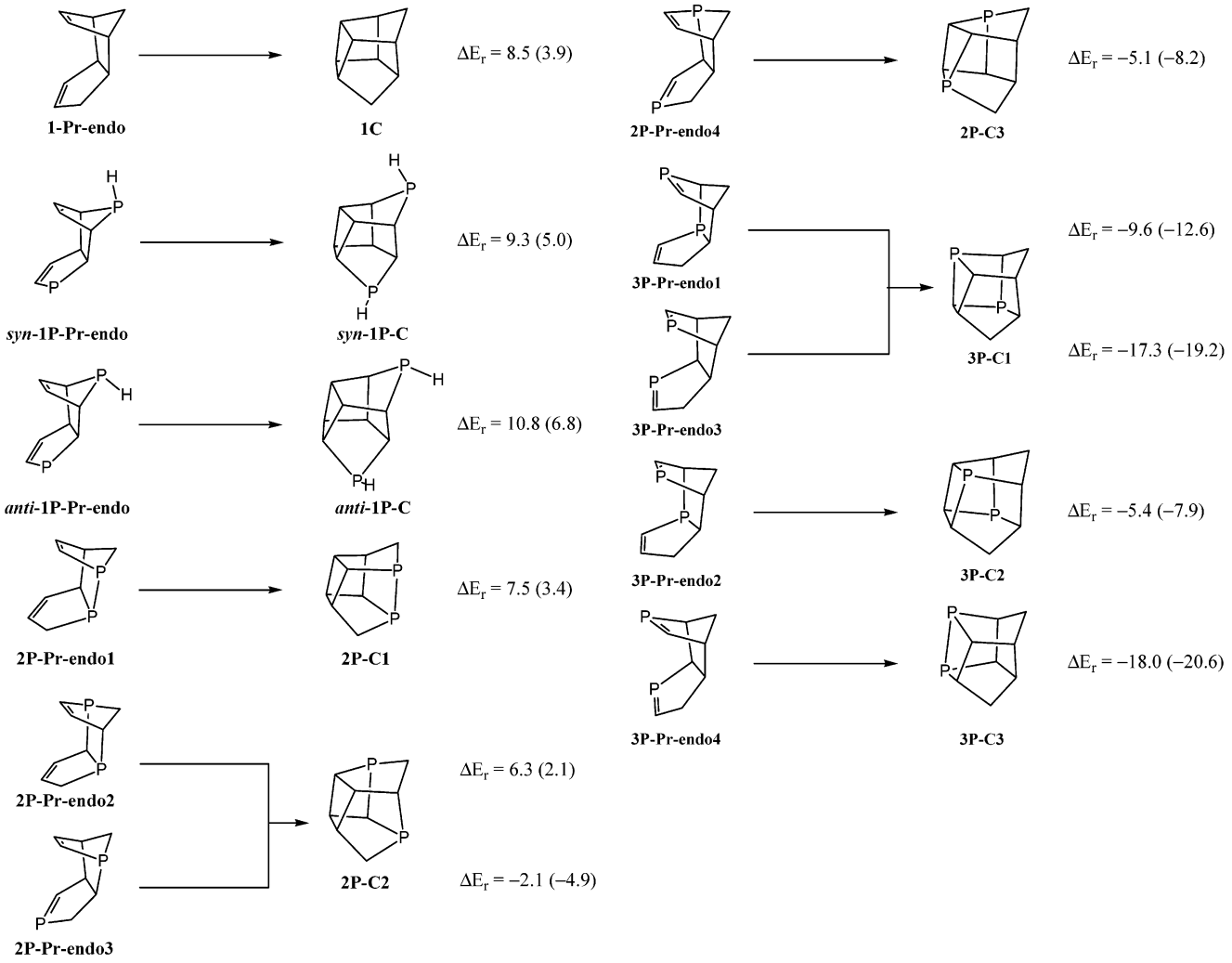

Figure 5. Reactions for the formation of cage compounds from endo dimers of phospholes as well as cyclopentadiene. Reaction energies obtained at the B3LYP/6-311+G** and B3LYP/6-31G* (in parentheses) levels are given. All the values are in kcal/mol.

for sigmatropic shifts between **2P** and **3P** are much higher compared to the corresponding activation barriers for the cyclodimerizations and the Diels–Alder reactions with dienophiles. It should be noted that the barriers for the formation of **exo4** and **endo4** products of **3P** are higher by about 4 kcal/mol than the conversion from **3P** to **2P**. Tables 1 and 3 indicate that the cyclodimerizations of **2P** and **3P** when the C=P part acts as a dienophile are more likely than the Diels–Alder reactions with ethylene or acetylene. Thus, the computational study indicates that cyclodimerization is a feasible reaction channel in phospholes, particularly in 2*H*- and 3*H*-phospholes.

After the cyclodimerizations, there are possibilities for further reaction, and two that obviously occurred to us are further cyclization to form cage structures and the possibility of trimerization. Only the endo products are suitable precursors for the formation of cage compounds; hence, they are taken as references. The reactions of the intramolecular cycloadditions for the formation of cage compounds from the endo Diels–Alder adducts considered in the present study are shown in Figure 5 along with the reaction energies. While the [2 + 2] cycloadditions are thermally forbidden reactions, the reaction exothermicities were previously employed for predicting the feasibility of cage formation.[36] The cage formation of all the **1P** dimers is endothermic, and therefore, these processes are not likely to take place. In contrast, all the **3P** dimers have high exothermicities for cage formation. Among the four **2P** dimers, two are exothermic and the other two are not.

Table 4 gives HOMO and LUMO energies and HOMO–LUMO energy gaps for the monomers and dimers as well as between the monomer and dimer obtained at the HF/6-31G* level. A closer look at the frontier molecular orbital energies of the monomers and dimers reveals the propensity for dimerizations as well as the possibility for further oligomerizations.[37] The origin of the higher reactivity of **2P** can be directly traced to the low HOMO–LUMO energy gap. Encouragingly, the frontier orbital energy differences nicely correlate with the reactivity, establishing that this class of dimerizations is orbital controlled. The HOMO–LUMO energy differences are consistently higher for the trimerization in 1*H*- and 2*H*-phospholes. However, the

(36) Mehta, G.; Padma, S.; Jemmis, E. D.; Leela, G.; Osawa, E.; Barbiric, D. A. *Tetrahedron Lett.* **1988**, *29*, 1613.
(37) Mehta, G.; Viswanath, M. B.; Sastry, G. N.; Jemmis, E. D.; Reddy, D. S. K.; Kunwar, A. C. *Angew. Chem., Int. Ed. Engl.* **1993**, *31*, 1488.

Table 4. HOMO and LUMO Energies (E_{HOMO} and E_{LUMO}) and HOMO−LUMO Energy Gaps (ΔE) for the Monomers and Dimers of Cyclopentadiene and Phospholes and also between the Monomer and Dimer Obtained at the HF/6-31G*//B3LYP/6-31G* Level[a]

structure	E_{HOMO}	E_{LUMO}	ΔE	ΔE_I[b]	ΔE_{II}[c]
1	−8.19	3.75	11.94		
1P	−8.70	2.76	11.46		
2P	−7.99	1.88	9.87		
3P	−8.44	2.20	10.64		
1-Pr-exo	−8.76	4.85	13.61	13.04	12.51
1-Pr-endo	−8.95	4.85	13.80	13.04	12.70
***syn*-1P-Pr-exo**	−8.45	3.59	12.04	12.29	11.21
***syn*-1P-Pr-endo**	−8.55	3.38	11.93	12.08	11.31
***anti*-1P-Pr-exo**	−8.81	3.66	12.47	12.36	11.56
***anti*-1P-Pr-endo**	−8.75	3.43	12.18	12.13	11.50
2P-Pr-exo1	−8.68	3.47	12.15	11.45	10.56
2P-Pr-endo1	−8.45	3.20	11.65	11.18	10.33
2P-Pr-exo2	−8.49	3.52	12.01	11.51	10.37
2P-Pr-endo2	−8.47	3.67	12.14	11.66	10.36
2P-Pr-exo3	−8.80	2.42	11.22	10.40	10.69
2P-Pr-endo3	−8.83	2.47	11.30	10.46	10.72
2P-Pr-exo4	−8.39	2.34	10.73	10.33	10.28
2P-Pr-endo4	−8.42	2.49	10.91	10.47	10.31
3P-Pr-exo1	−8.64	2.28	10.92	10.71	10.84
3P-Pr-endo1	−8.35	2.32	10.67	10.75	10.55
3P-Pr-exo2	−8.32	2.21	10.53	10.65	10.51
3P-Pr-endo2	−8.08	2.30	10.38	10.74	10.28
3P-Pr-exo3	−8.58	2.24	10.82	10.68	10.77
3P-Pr-endo3	−8.61	2.19	10.80	10.62	10.81
3P-Pr-exo4	−8.70	2.29	10.99	10.72	10.90
3P-Pr-endo4	−8.47	2.13	10.60	10.56	10.66

[a] All the values are in eV. [b] $\Delta E_I = E_{HOMO}$(monomer) − E_{LUMO}(dimer). [c] $\Delta E_{II} = E_{HOMO}$(dimer) − E_{LUMO}(monomer).

energy differences are quite similar for the dimerization and trimerization of 3*H*-phosphole. Therefore, in the conditions favorable for dimerizations, the trimerizations should also be feasible.

Conclusions

The present study reports first systematic computational study for all the possible dimerizations of phospholes through [4 + 2] cycloaddition at the B3LYP level. The activation energies reveal that endo fusion is more preferred over exo. The reaction energies indicate that exo dimers are more stable than endo dimers in **2P** and **3P** and the cyclopentadiene dimerizations. The very low activation energy and high exothermicity for the formation of the P−P-bonded **2P** dimer among the **2P** dimerizations support Mathey's experimental observation of only this dimer, and the computations also support the experimental observation that the exo product is more stable than the endo product.[4] The high reactivity of 2*H*- and 3*H*-phospholes can be traced to the conversion of weak C−P double bonds to single bonds during the cyclization. In cases where the C═C bonds are involved, the dimerization energies are comparable to those observed in the cyclopentadiene reaction. The transition-state geometries indicate that all the transition states are nonsynchronous in nature, although the reactions are concerted. Comparison of the activation energies for cyclodimerizations, sigmatropic shifts, and the Diels−Alder reactions with ethylene and acetylene as dienophiles indicate that dimerization is a very competent pathway, especially for 2*H*- and 3*H*-phospholes. The consequent reactions of the dimerizations have also been explored. 1*H*-Phosphole dimers did not show the possibility for either cage formation or further oligomerization. In contrast, not only were 3*H*-phospholes found to be reactive for dimerization but also the dimers formed were found to show high propensity for cage formation as well as for further oligomerization. The reactivity of the thermodynamically more stable 2*H*-phosphole (**2P**) is the highest. Thus, the present study demonstrates that the cyclodimerization and consequent reaction channels are the stumbling blocks for the isolation of 3*H*-phospholes. 1*H*- and 2*H*-phospholes are expected to form stable dimers. The present computational study indicates that the controlled dimerization pathway may be effectively employed to access novel polycyclic organophosphorus compounds.

Acknowledgment. T.C.D. thanks the CSIR, New Delhi, India, for a senior research fellowship. Dr. J. S. Yadav, Director, IICT, is thanked for encouragement and support. Mr. M. Elango is thanked for assistance in doing preliminary calculations.

Supporting Information Available: Figures showing HOMO−LUMO interactions and tables giving total energies, the B3LYP/6-31G* optimized Cartesian coordinates of the monomers, transition states and products of dimers and the cage compounds, and frontier orbital energies. This material is available free of charge via the Internet at http://pubs.acs.org.

OM0340490